An Approach to Heterometallic Complexes with Selenolate and Tellurolate Ligands: Crystal Structures of *cis*-$[Mn(CO)_4(SePh)_2]^-$, $[(CO)_3Mn(\mu\text{-}SeMe)_3Mn(CO)_3]^-$, $(CO)_4Mn(\mu\text{-}TePh)_2Co(CO)(\mu\text{-}SePh)_3Mn(CO)_3$, and $(CO)_3Mn(\mu\text{-}SePh)_3Fe(CO)_3$

Wen-Feng Liaw,*,† Chih-Yuan Chuang,† Way-Zen Lee,† Chen-Kang Lee,† Gene-Hsiang Lee,‡ and Shie-Ming Peng‡

Departments of Chemistry, National Changhua University of Education, Changhua, Taiwan 50058, ROC, and National Taiwan University, Taipei, Taiwan 10764, ROC

Received November 20, 1995[⊗]

Oxidative addition of diorganyl diselenides to the coordinatively unsaturated, low-valent transition-metal−carbonyl fragment $[Mn(CO)_5]^-$ produced *cis*-$[Mn(CO)_4(SeR)_2]^-$. The complex *cis*-[PPN][$Mn(CO)_4(SePh)_2$] crystallized in triclinic space group $P\bar{1}$ with $a = 10.892(8)$ Å, $b = 10.992(7)$ Å, $c = 27.021(4)$ Å, $\alpha = 101.93(4)°$, $\beta = 89.79(5)°$, $\gamma = 116.94(5)°$, $V = 2807(3)$ Å^3, and $Z = 2$; final $R = 0.085$ and $R_w = 0.094$. Thermolytic transformation of *cis*-$[Mn(CO)_4(SeMe)_2]^-$ to $[(CO)_3Mn(\mu\text{-}SeMe)_3Mn(CO)_3]^-$ was accomplished in high yield in THF at room temperature. Crystal data for [Na-18-crown-6-ether][$(CO)_3Mn(\mu\text{-}SeMe)_3Mn(CO)_3$]: trigonal space group $R\bar{3}$, $a = 13.533(3)$ Å, $c = 32.292(8)$ Å, $V = 5122(2)$ Å^3, $Z = 6$, $R = 0.042$, $R_w = 0.041$. Oxidation of Co^{2+} to Co^{3+} by diphenyl diselenide in the presence of chelating metallo ligands *cis*-$[Mn(CO)_4(SePh)_2]^-$ and *cis*-$[Mn(CO)_4(TePh)_2]^-$, followed by a bezenselenolate ligand rearranging to bridge two metals and a labile carbonyl shift from Mn to Co, led directly to $[(CO)_4Mn(\mu\text{-}TePh)_2Co(CO)(\mu\text{-}SePh)_3Mn(CO)_3]$. Crystal data: triclinic space group $P\bar{1}$, $a = 11.712(3)$ Å, $b = 12.197(3)$ Å, $c = 15.754(3)$ Å, $\alpha = 83.56(2)°$, $\beta = 76.13(2)°$, $\gamma = 72.69(2)°$, $V = 2083.8(7)$ Å^3, $Z = 2$, $R = 0.040$, $R_w = 0.040$. Addition of *fac*-$[Fe(CO)_3(SePh)_3]^-$ to *fac*-$[Mn(CO)_3(CH_3CN)_3]^+$ resulted in formation of $(CO)_3Mn(\mu\text{-}SePh)_3Fe(CO)_3$. This neutral heterometallic complex crystallized in monoclinic space group $P2_1/n$ with $a = 8.707(2)$ Å, $b = 17.413(4)$ Å, $c = 17.541(4)$ Å, $\beta = 99.72(2)°$, $V = 2621(1)$ Å^3, and $Z = 4$; final $R = 0.033$ and $R_w = 0.030$.

Introduction

Recent work in this laboratory has focused on the syntheses and characterizations of novel metal tellurolate and selenolate complexes via activation of diorganyl dichalcogenides (oxidative addition/nucleophilic displacement) to anionic metallic fragments. Application of anionic metallic fragments for preparation of metal tellurolates/selenolates has been proved to be one of the most versatile routes and to be particularly suitable for d^8 anionic metal carbonyls ($[HFe(CO)_4]^-$, $[REFe(CO)_4]^-$ (E = Se, Te; R = Ph, alkyl), $[Mn(CO)_5]^-$, $[Re(CO)_5]^-$).[1,2] There have been many reports relevant to the syntheses of metal selenolate and tellurolate complexes. Synthetic approaches, to our knowledge, involve the protolysis including reaction of alkylmetal/metal amido complexes with selenol/tellurol,[3] the metathesis or transmetalation between an alkali-metal selenolate and a metal halide,[4] insertion,[5] nucleophilic cleavage of the E−E (E = Se, Te) bonds by metal hydrides,[1] and the oxidation of metal upon reaction with the diorganyl dichalcogenides.[1,2,6]

Interest in metal chalcogenolates stems not only from their potential use as precursors for M/Se materials[7] but also from the perspective of reactivity. In particular, the use of the complexes *cis*-$[Mn(CO)_4(ER)_2]^-$ and *fac*-$[Fe(CO)_3(EPh)_3]^-$ (E = Se, Te) is of further interest because they contain sites of latent reactivity, the delocalized lone pairs of electrons around chalcogen atoms, which may react with other organometallic moieties to form heterometallic chalcogenolate species. In our continued work on transition-metal chalcogenolates, we have concentrated our attention on the development of heterometallic chalcogenolate species and a synthetic route to new metal−chalcogenolate species employing *cis*-$[Mn(CO)_4(ER)_2]^-$ and *fac*-$[Fe(CO)_3(EPh)_3]^-$ as chelating ligands and intermetal ligand transfer reagents.

In this paper it is shown that the anionic $[Mn(CO)_5]^-$ is effective in activating the Se−Se bond of diorganyl diselenides and that *cis*-$[Mn(CO)_4(ER)_2]^-$ and *fac*-$[Fe(CO)_3(SePh)_3]^-$ are potential "chelating metallo ligands" in the syntheses of

† National Changhua University of Education.
‡ National Taiwan University.
⊗ Abstract published in *Advance ACS Abstracts,* March 15, 1996.

(1) (a) Liaw, W.-F.; Chiang, M.-H.; Liu, C.-J.; Harn, P.-J.; Liu, L.-K. *Inorg. Chem.* **1993**, *32*, 1536. (b) Liaw, W.-F.; Lai, C.-H.; Lee, C.-K.; Lee, G.-H.; Peng, S.-M. *J. Chem. Soc., Dalton Trans.* **1993**, 2421. (c) Liaw, W.-F.; Lai, C.-H.; Chiang, M.-H.; Hsieh, C.-K.; Lee, G.-H.; Peng, S.-M. *J. Chin. Chem. Soc. (Taipei)* **1993**, *40*, 437. (d) Liaw, W.-F.; Ou, D.-S.; Horng, Y.-C.; Lai, C.-H.; Lee, G.-H.; Peng, S.-M. *Inorg. Chem.* **1994**, *33*, 2495. (e) Liaw, W.-F.; Chiou, S.-J.; Lee, W.-Z.; Lee, G.-H.; Peng, S.-M. *J. Chin. Chem. Soc. (Taipei)* **1993**, *40*, 361.

(2) Liaw, W.-F.; Ou, D.-S.; Li, Y.-S.; Lee, W.-Z.; Chuang, C.-Y.; Lee, Y.-P.; Lee, G.-H.; Peng, S.-M. *Inorg. Chem.* **1995**, *34*, 3747.

(3) (a) Cary, D. R.; Ball, G. E.; Arnold, J. *J. Am. Chem. Soc.* **1995**, *117*, 3492. (b) Bochmann, M.; Powell, A. K.; Song, X. *J. Chem. Soc., Dalton Trans.* **1995**, 1645. (c) Ellison, J. J.; Ruhlandt-Senge, K.; Hope, H. H.; Power, P. P. *Inorg. Chem.* **1995**, *34*, 49. (d) Ruhlandt-Senge, K.; Power, P. P. *Inorg. Chem.* **1993**, *32*, 3478. (e) Gindelberger, D. E.; Arnold, J. *Inorg. Chem.* **1994**, *33*, 6293. (f) Ruhlandt-Senge, K. *Inorg. Chem.* **1995**, *34*, 3499. (g) Strzelecki, A. R.; Likar, C. L.; Helsel, B. A.; Utz, T.; Lin, M. C.; Bianconi, P. A. *Inorg. Chem.* **1994**, *33*, 5188. (h) Cary, D. R.; Arnold, J. *Inorg. Chem.* **1994**, *33*, 1791.

(4) (a) Kersting, B.; Krebs, B. *Inorg. Chem.* **1994**, *33*, 3886. (b) Berardini, M.; Emge, T.; Brennan, J. G. *J. Am. Chem. Soc.* **1993**, *115*, 8501. (c) Ruhlandt-Senge, K.; Davis, K.; Dalal, S.; Englich, U.; Senge, M. O. *Inorg. Chem.* **1995**, *34*, 2587.

(5) (a) Eikens, W.; Kienitz, C.; Jones, P. G.; Thöne, C. *J. Chem. Soc. Dalton Trans.* **1994**, 3329. (b) Christuk, C. C.; Ibers, J. A. *Inorg. Chem.* **1993**, *32*, 5105.

(6) (a) Brewer, M.; Khasnis, D.; Buretea, M.; Berardini, M.; Emge, T. J.; Brennan, J. G. *Inorg. Chem.* **1994**, *33*, 2743. (b) Lee, J.; Brewer, M.; Berardini, M.; Brennan, J. G. *Inorg. Chem.* **1995**, *34*, 3215.

(7) (a) Kanatzidis, M. G.; Huang, S. *Coord. Chem. Rev.* **1994**, *130*, 509. (b) Brennan, J. G.; Siegrist, T.; Carroll, P. J.; Stuczynski, S. M.; Brus, L. E.; Steigerwald, M. L. *J. Am. Chem. Soc.* **1989**, *111*, 4141.

0020-1669/96/1335-2530$12.00/0

heterometallic chalcogenolates. Specifically, the syntheses and characterizations of the novel *cis*-$[Mn(CO)_4(SePh)_2]^-$, **1**, the triply-bridged selenolate complex $[(CO)_3Mn(\mu\text{-}SeMe)_3Mn(CO)_3]^-$, **2**, and a heterometallic Mn(I)−Co(III)−Mn(I) mixed-chalcogenolate complex $(CO)_4Mn(\mu\text{-}TePh)_2Co(CO)(\mu\text{-}SePh)_3Mn(CO)_3$, **3**, from reduction of diphenyl diselenide by Co^{2+} in the presence of chelating metallo ligands *cis*-$[Mn(CO)_4(EPh)_2]^-$ (E = Se, Te) are described. In addition, the synthesis and structure of the isolobal species $(CO)_3Mn(\mu\text{-}SePh)_3Fe(CO)_3$, **4**, are reported. Also, we provide more mechanistic information about the formation of *cis*-$[Mn(CO)_4(SeR)_2]^-$.

Experimental Section

Manipulations, transfers, and reactions of samples were conducted under nitrogen according to standard Schlenk techniques or in a glovebox (Ar gas). Solvents were distilled under nitrogen from appropriate drying agents (diethyl ether from CaH_2; acetonitrile from CaH_2/P_2O_5; hexane and tetrahydrofuran (THF) from Na/benzophenone) and stored in dried, N_2-filled flasks over 4 Å molecular sieves. A nitrogen purge was used on these solvents before use, and transfers to reaction vessels were via stainless-steel cannula under N_2 at a positive pressure. The reagents manganese decacarbonyl, 18-crown-6-ether, tellurium powder, diphenyl diselenide, bis(triphenylphosphoranylidene)-ammonium chloride, phenylmagnesium bromide, dimethyl diselenide, iron pentacarbonyl, and cobalt perchlorate (Aldrich) were used as received. Infrared spectra were recorded on a spectrometer (Bio-Rad FTS-7 FTIR) with sealed solution cells (0.1 mm) and KBr windows. In NMR spectra (recorded on a Bruker AC 200 spectrometer), chemical shifts of ^1H and ^{13}C are relative to tetramethylsilane. UV−visible spectra were recorded on a GBC 918 spectrophotometer. Gas chromatography was carried out on a Varian 3300 using a Shimadzu RC-6A integrator. Analyses made use of a flame ionizing detector (FID); nitrogen was the carrier gas, the column was OV-17 (5%) on Chromosorb W, 80/100 mesh, 6 ft × $^1/_8$ in. stainless steel tubing. Analyses of carbon, hydrogen, and nitrogen were obtained with a CHN analyzer (Heraeus).

Preparation of *cis*-[PPN][Mn(CO)$_4$(SePh)$_2$]. [PPN][$Mn(CO)_5$] (0.5 mmol, 0.367 g)[8] dissolved in THF (5 mL) was stirred under N_2, and diphenyl diselenide (0.5 mmol, 0.156 g) in THF solution was added to the [PPN][$Mn(CO)_5$] solution by cannula under positive N_2 gas at room temperature. A vigorous reaction occurred immediately with evolution of CO gas. After stirring of the reaction solution for 0.5 h, the volume of the solution was reduced to 3 mL and an orange-yellow product precipitated on addition of hexane (20 mL) at 0 °C. The product was isolated by removing the solvent and recrystallized from THF−hexane under CO atmosphere. The yield was 0.48 g (95%) of an orange-yellow solid *cis*-[PPN][$Mn(CO)_4(SePh)_2$]. The orange-yellow solution was layered with hexane under CO atmosphere; storage for 4 weeks at −10 °C led to formation of orange-yellow crystals *cis*-[PPN][$Mn(CO)_4(SePh)_2$] suitable for X-ray crystallography. IR (ν_{CO}) (THF): 2041 m, 1969 vs, 1950 m, 1908 m cm^{-1}. ^1H NMR (CD_3CN): δ 6.9−7.7 (m) ppm. ^{13}C NMR (CD_3CN): δ 137.0, 134.5, 133.1, 130.2, 129.2, 128.4, 127.1, 124.9 ppm. Absorption spectrum (THF) [λ_{max}, nm (ϵ, M^{-1} cm^{-1})]: 438 (1660), 364 (2219), 290 (23 139). Anal. Calcd for $C_{52}H_{40}O_4NP_2Se_2Mn$: N, 1.38; C, 61.37; H, 3.96. Found: N, 1.54; C, 61.04; H, 4.05.

Preparation of [PPN][$(CO)_3Mn(\mu\text{-}SePh)_3Mn(CO)_3$]. *cis*-[PPN]-[$Mn(CO)_4(SePh)_2$] (0.5 mmol, 0.509 g) in 20 mL of THF was heated at 60 °C under nitrogen for 6 h. When the solution was cooled to room temperature, the volume of the solution was reduced to 10 mL under vacuum and diethyl ether (10 mL) was added. The red-brown solution was filtered to remove [PPN][SePh], and recrystallization from THF−diethyl ether (1:2 ratio) gave an orange-brown solid [PPN]-[$(CO)_3Mn(\mu\text{-}SePh)_3Mn(CO)_3$]. The yield was 0.285 g (88.7%). IR (ν_{CO}) (THF): 1981 s, 1902 vs cm^{-1}. ^1H NMR (CD_3CN): δ 7.0−7.9 (m) (Ph) ppm. Absorption spectrum (THF) [λ_{max}, nm (ϵ, M^{-1} cm^{-1})]: 409 (2768), 312 (7704), 273 (20 128). Anal. Calcd for $C_{60}H_{45}O_6NP_2Se_3Mn_2$: N, 1.09; C, 56.09; H, 3.53. Found: N, 1.43; C, 56.08; H, 3.81.

Addition of [Na-18-crown-6-ether][$Mn(CO)_5$] and $(MeSe)_2$. [Na-18-crown-6-ether][$Mn(CO)_5$] (0.5 mmol, 0.291 g)[8] and $(MeSe)_2$ (0.094 g, 0.5 mmol) dissolved in 10 mL of THF were stirred under nitrogen at ambient temperature. A vigorous reaction occurred immediately with evolution of CO gas. The reaction was monitored with FTIR constantly. The IR spectrum, ν_{CO} (THF) 2031 m, 1960 vs, 1938 m, 1894 m cm^{-1}, having the same pattern as but differing slightly in position from that of *cis*-$[Mn(CO)_4(SePh)_2]^-$, indicated the formation of *cis*-$[Mn(CO)_4(SeMe)_2]^-$. ^1H NMR (CD_3CN): δ 1.53 (s) ppm (CH_3) for *cis*-[Na-18-crown-6-ether][$Mn(CO)_4(SeMe)_2$]. The reaction mixture was stirred for 1 h at room temperature; the IR spectrum showed two new bands attributed to carbonyl stretching modes (ν_{CO} (THF) 1969 vs, 1886 vs cm^{-1}) of [Na-18-crown-6-ether][$(CO)_3Mn(\mu\text{-}SeMe)_3Mn(CO)_3$]. The reaction solution was stirred at room temperature for 5 h; the IR spectrum revealed that all *cis*-$[Mn(CO)_4(SeMe)_2]^-$ had completely converted to [Na-18-crown-6-ether][$(CO)_3Mn(\mu\text{-}SeMe)_3Mn(CO)_3$]. The reaction mixture was reduced to 5 mL under vacuum, and diethyl ether (5 mL) was added. The solution was then filtered to remove [Na-18-crown-6-ether][MeSe]. The orange-brown solution was layered with hexane; storage for 3 weeks at −10 °C led to formation of orange-brown crystals of [Na-18-crown-6-ether][$(CO)_3Mn(\mu\text{-}SeMe)_3Mn(CO)_3$] suitable for X-ray crystallography. ^1H NMR (CD_3CN): δ 1.75 (CH_3) (satellite $J_{^1H-^{77}Se}$ = 8.6 Hz), 3.6 (s) ppm (18-crown-6-ether). ^{13}C NMR (CD_3CN): δ 26.2 (s) ppm (CH_3). IR (ν_{CO}) (THF): 1969 s, 1886 vs cm^{-1}.

Preparation of $(CO)_3Mn(\mu\text{-}SePh)_3Co(CO)(\mu\text{-}TePh)_2Mn(CO)_4$. The reaction mixture, *cis*-[PPN][$Mn(CO)_4(SePh)_2$] (0.204 g, 0.2 mmol) and *cis*-[PPN][$Mn(CO)_4(TePh)_2$] (0.223 g, 0.2 mmol), was added to $Co(ClO_4)_2\cdot 6H_2O$ (73.2 mg, 0.2 mmol) and $(PhSe)_2$ (41 mg, 0.1 mmol) in THF solution. After 10 min of stirring at room temperature, the solvent was removed at reduced pressure. The residue was dissolved in 35 mL of diethyl ether at 0 °C, and the dark purple solution was filtered to remove [PPN][ClO_4]. The filtrate (in diethyl ether) was stored in a refrigerator (−10 °C) for 3 weeks to induce precipitation of dark purple crystals of $(CO)_3Mn(\mu\text{-}SePh)_3Co(CO)(\mu\text{-}TePh)_2Mn(CO)_4$; yield 0.228 g (90%). IR (ν_{CO}) (THF): 2063 w, 2027 sh, 2007 vs, 1988 m, 1959 w, 1928 m cm^{-1}. ^1H NMR (C_4D_8O): δ 6.95−8.24 (m) ppm (Ph). ^{13}C NMR (C_4D_8O): δ 138.4, 137.1, 137.0, 136.3, 135.2, 130.2, 129.9, 129.7, 129.5, 129.2, 129.0. Anal. Calcd for $C_{38}H_{25}O_8Te_2Se_3CoMn_2$: C, 35.93; H. 1.98. Found: C, 36.73; H, 2.16.

Safety Note. *Perchlorate salts of metal complexes with organic ligands are potentially explosive. Only small amounts of material should be prepared, and these should be handled with great caution.*

Reaction of PhSeBr and [PPN][$Mn(CO)_5$]. [PPN][$Mn(CO)_5$] (0.147 g, 0.2 mmol)[8] was added to PhSeBr (47.2 mg, 0.2 mmol) in THF (5 mL) around −20 °C. A vigorous reaction occurred immediately and was monitored with FTIR. The IR spectrum, ν_{CO} (THF) 2116 w, 2027 s, 2000 m cm^{-1}, having the same pattern as but differing slightly in position from that of $PhTeRe(CO)_5$ (IR (ν_{CO}) (THF): 2128 w, 2024 s, 1986 m cm^{-1}),[9] indicated the formation of $PhSeMn(CO)_5$. The reaction mixture was stirred for 4 h at ambient temperature; the IR spectrum showed four new bands attributed to the well-known carbonyl stretching modes of $Mn_2(\mu\text{-}SePh)_2(CO)_8$.[9,10] IR ($\nu_{CO}$) (THF): 2065 m, 2012 vs, 1998 m, 1962 s cm^{-1}.

Reaction of [PPN][$Mn(CO)_4(SePh)_2$] and $NOPF_6$. A solution containing 0.102 g (0.1 mmol) of [PPN][$Mn(CO)_4(SePh)_2$] and 35 mg (0.2 mmol) of $NOPF_6$ in acetonitrile (10 mL) was stirred under nitrogen overnight at room temperature. The green-orange solution was dried under vacuum; THF−diethyl ether (2:1 ratio) was added to the residue, and the mixture was filtered to remove the insoluble solid. The green-orange solution was dried again under vacuum, and THF−hexane (1:10 ratio) was added to precipitate the known pale yellow solid *fac*-[$Mn(CO)_3(CH_3CN)_3$][PF_6].[11] IR (ν_{CO}) (THF): 2060 m, 1970 vs cm^{-1}. ^1H NMR (CD_3CN): δ 2.31 (s) ppm (CH_3CN) (free CH_3CN is noted at 1.94 (s) ppm).

(8) Inkrott, K.; Goetze, G.; Shore, S. G. *J. Organomet. Chem.* **1978**, *154*, 337.
(9) Liaw, W.-F.; Horng, Y.-C.; Ou, D.-S.; Chuang, C.-Y.; Lee, C.-K.; Lee, G.-H.; Peng, S.-M. *J. Chin. Chem. Soc. (Taipei)* **1995**, *42*, 59.
(10) Chaudhuri, M. K.; Hass, A.; Wensky, A. *J. Organomet. Chem.* **1976**, *116*, 323.

Table 1. Crystallographic Data for Complexes **1** and **2**

	1	**2**
empirical formula	$C_{60}H_{56}O_6NP_2MnSe_2$	$C_{23}H_{39}O_{14}Mn_2Se_3Na$
fw	1161.90	1017.13
cryst syst	triclinic	trigonal
space group	$P\bar{1}$	$R\bar{3}$
λ, Å (Mo Kα)	0.7107	0.7107
a, Å	10.892(8)	13.533(3)
b, Å	10.992(7)	
c, Å	27.021(4)	32.292(8)
α, deg	101.93(4)	
β, deg	89.79(5)	
γ, deg	116.94(5)	
V, Å^3	2807(3)	5122(2)
Z	2	6
ρ_{calcd}, g cm^{-3}	1.375	1.769
μ, cm^{-1}	16.1	59.3
T, °C	25	25
R^a	0.085	0.042
$R_w{}^b$	0.094	0.041

^{a} $R = \sum|F_o - F_c|/\sum F_o$. ^{b} $R_w = [\sum w(F_o - F_c)^2/\sum wF_o^2]^{1/2}$.

Reaction of *cis*-[Mn(CO)$_4$(SePh)$_2$]$^-$ and I$_2$. A solution of I_2 (51 mg, 0.2 mmol) in THF (5 mL) was added dropwise to *cis*-[PPN][Mn(CO)$_4$(SePh)$_2$] (0.204 g, 0.2 mmol) in THF solution under nitrogen at ambient temperature. The solution was dried under vacuum, and hexane was added to extract the green-yellow product $(SePh)_2$ identified by ^{1}H NMR and GC. The residue was identified as the well-known *cis*-[Mn(CO)$_4$(I)$_2$]$^-$ product.[12] IR (ν_{CO}) (THF): 2066 w, 1994 s, 1971 m, 1927 m cm^{-1}. *cis*-[Mn(CO)$_4$(I)$_2$]$^-$ was also obtained by dropwise addition of I_2 to [PPN][Mn(CO)$_5$] in THF.

Preparation of (CO)$_3$Mn(μ-SePh)$_3$Fe(CO)$_3$. *fac*-[PPN][Fe(CO)$_3$(SePh)$_3$] (0.573 g, 0.5 mmol) in 5 mL of THF was slowly added to a stirred THF solution of *fac*-[Mn(CO)$_3$(CH$_3$CN)$_3$][PF$_6$] (0.2035 g, 0.5 mmol)[11] at ambient temperature. The reaction mixture was allowed to stir for 3 h at room temperature. The solution was concentrated to 1 mL, and diethyl ether was added to extract the brown-red product by filtering to remove [PPN][PF$_6$]. The solution was then dried under vacuum, and diethyl ether−hexane (1:2 ratio) was added to extract the pure dark red-brown product. Upon removal of diethyl ether−hexane in vacuum, dark red-brown solid (CO)$_3$Mn(μ-SePh)$_3$Fe(CO)$_3$ (0.220 g, 59%) was obtained. Crystals suitable for X-ray diffraction were grown from diethyl ether at −10 °C. IR (ν_{CO}) (THF): 2081 s, 2031 sh, 2017 vs, 1931 s cm^{-1}. ^{1}H NMR (CD$_3$CN): δ 7.27−8.02 (m) ppm. ^{13}C NMR (CD$_3$CN): δ 126.9, 130.0, 130.2, 132.2, 135.3, 203.2, 171.6 ppm. Anal. Calcd for $C_{24}H_{15}O_6Se_3MnFe$: C, 38.59; H, 2.02. Found: C, 38.34; H, 2.40.

Crystallography. The crystal data are summarized in Tables 1 and 2. The crystal of **1** moderately sensitive to air chosen for diffraction measurement was *ca*. 0.20 × 0.25 × 0.50 mm; the orange-red crystal of **2** had dimensions 0.40 × 0.50 × 5.00 mm; the dark purple crystal of **3** had dimensions 0.05 × 0.40 × 0.40 mm; the crystal of **4** that was extremely sensitive to light and heat was 0.30 × 0.35 × 0.50 mm. Each crystal was mounted on a glass fiber and quickly coated in epoxy resin. The unit-cell parameters were obtained from 25 reflections with 2θ between 14.90 and 21.42° for product **1**; the ranges were 15.20 ° < 2θ < 24.52° for product **2**, 15.64° < 2θ < 24.66° for product **3**, and 16.32° < 2θ < 24.24° for product **4**. Diffraction measurements were carried out on a Nonius CAD 4 diffractometer with graphite-monochromated Mo Kα radiation employing the $\theta/2\theta$ scan mode. A φ scan absorption correction was made. Structural determinations were made using the NRCC-SDP-VAX package of programs.[13] Selected bond distances and angles are listed in Tables 3 and 4. Fractional atomic coordinates and B_{eq} values (Å^2) of complexes **1**−**4** are listed in Tables 5−8.

Table 2. Crystallographic Data for Complexes **3** and **4**

	3	**4**
empirical formula	$C_{38}H_{25}O_8CoMn_2Se_3Te_2$	$C_{24}H_{15}O_6MnSe_3Fe$
fw	1270.49	747.04
cryst syst	triclinic	monoclinic
space group	$P\bar{1}$	$P2_1/n$
λ, Å(Mo Kα)	0.7107	0.7107
a, Å	11.712(3)	8.7066(16)
b, Å	12.197(3)	17.413(4)
c, Å	15.754(3)	17.541(4)
α, deg	83.558(18)	
β, deg	76.133(17)	99.718(18)
γ, deg	72.686(18)	
V, Å^3	2083.8(7)	2621.2(10)
Z	2	4
ρ_{calcd}, g cm^{-3}	2.025	1.893
μ, cm^{-1}	50.0	26.7
T, °C	25	25
R^a	0.040	0.033
$R_w{}^b$	0.040	0.030

^{a} $R = \sum|F_o - F_c|/\sum F_o$. ^{b} $R_w = [\sum w(F_o - F_c)^2/\sum wF_o^2]^{1/2}$.

Table 3. Selected Bond Distances (Å) and Angles (deg) for **1** and **2**

(a) *cis*-[PPN][Mn(CO)$_4$(SePh)$_2$]

Se(1)−Mn	2.529(4)	Mn−C(1)	1.736(24)
Se(2)−Mn	2.524(4)	Mn−C(2)	1.776(21)
Se(1)−C(5)	1.970(17)	Mn−C(3)	1.805(22)
Se(2)−C(11)	1.952(19)	Mn−C(4)	1.799(22)
Se(1)−Mn−Se(2)	82.97(13)	Se(1)−Mn−C(1)	86.7(8)
Mn−Se(1)−C(5)	104.1(5)	Se(1)−Mn−C(2)	91.5(7)
Mn−Se(2)−C(11)	105.6(6)	Se(1)−Mn−C(3)	177.7(7)
C(2)−Mn−C(4)	94.1(11)	Se(1)−Mn−C(4)	86.6(7)
C(2)−Mn−C(3)	90.7(10)	C(1)−Mn−C(4)	167.5(12)
C(1)−Mn−C(2)	96.5(12)	C(1)−Mn−C(3)	92.6(11)
C(3)−Mn−C(4)	93.7(11)		

(b) [Na-18-crown-6-ether][(CO)$_3$Mn(μ-SeMe)$_3$Mn(CO)$_3$]

Se−Mn(1)	2.508(2)	Se−Mn(2)	2.494(2)
Se−C(3)	1.981(8)		
Mn(1)−Se−C(3)	108.1(3)	Se−Mn(2)−Se	81.79(6)
Mn(2)−Se−C(3)	106.9(3)	Se−Mn(1)−C(1)	95.2(3)
Mn(1)−Se−Mn(2)	82.15(6)	Se−Mn(1)−C(1)	91.9(4)
Se−Mn(1)−Se	81.23(6)	Se−Mn(1)−C(1)	172.7(2)

Results and Discussion

The chemistry reported herein is summarized in Scheme 1. The reaction of diphenyl diselenide with [Mn(CO)$_5$]$^-$ proceeds cleanly in dry THF to form *cis*-[Mn(CO)$_4$(SePh)$_2$]$^-$ via an oxidative decarbonylation addition at room temperature (Scheme 1a). This is in contrast to the reaction with [Re(CO)$_5$]$^-$, which forms neutral PhSeRe(CO)$_5$.[14] The nature of the metal fragment environment clearly plays a critical role in determining the course of these reactions. In contrast to oxidative addition of diphenyl diselenide to [Mn(CO)$_5$]$^-$, reaction of [Mn(CO)$_5$]$^-$ with PhSeBr in THF at 0 °C proceeded in surprising fashion to give the monomeric species PhSeMn(CO)$_5$ as the initial product according to IR (ν_{CO}) spectra (Scheme 1c).[9,15] The monomeric PhSeMn(CO)$_5$ was unstable with respect to CO loss and dimerization when the reaction mixture was allowed to stir at room temperature (Scheme 1d). The dimerization or transformation product (CO)$_4$Mn(μ-SePh)$_2$Mn(CO)$_4$ was well-known and identified by ^{1}H NMR and IR.[9,10]

An atmosphere of CO failed to prevent oxidative addition of PhSeSePh even when we exposed the mixture of [Mn(CO)$_5$]$^-$ and $(PhSe)_2$ to 1 atm of CO in THF at room temperature. The hexane-insoluble *cis*-[Mn(CO)$_4$(SePh)$_2$]$^-$ was recrystallized as

(11) Drew, D.; Darensbourg, D. J.; Darensbourg, M. Y. *Inorg. Chem.* **1975**, *14*, 1579.
(12) Abel, E. W.; Wilkinson, G. *J. Chem. Soc.* **1959**, 1501.
(13) Gabe, E. J.; LePage, Y.; Chrarland, J. P.; Lee, F. L.; White, P. S. *J. Appl. Crystallogr.* **1989**, *22*, 384.
(14) Liaw, W.-F.; Lee, W.-Z. Unpublished results.
(15) Osborne, A. G.; Stone, F. G. A. *J. Chem. Soc. A* **1966**, 1143.

Table 4. Selected Bond Distances (Å) and Angles (deg) for **3** and **4**

(a) $(CO)_4Mn(\mu\text{-}TePh)_2Co(CO)(\mu\text{-}SePh)_3Mn(CO)_3$

Te(1)−Co	2.581(2)	Te(1)−Mn(2)	2.678(2)
Te(2)−Co	2.570(2)	Te(2)−Mn(2)	2.630(2)
Se(1)−Co	2.476(2)	Se(1)−Mn(1)	2.530(2)
Se(2)−Co	2.429(2)	Se(2)−Mn(1)	2.503(2)
Se(3)−Co	2.444(2)	Se(3)−Mn(1)	2.524(2)
Co−C(1)	1.761(10)	C(1)−O(1)	1.136(12)
Mn(2)−C(5)	1.860(11)	Mn(1)−C(2)	1.784(11)
Mn(2)−C(6)	1.796(12)	Mn(1)−C(3)	1.762(12)
Mn(2)−C(7)	1.844(11)	Mn(1)−C(4)	1.791(11)
Mn(2)−C(8)	1.798(12)		

Co−Te(1)−Mn(2)	93.59(6)	Co−Te(1)−C(9)	108.5(3)
Co−Te(2)−Mn(2)	94.99(6)	Co−Te(2)−C(15)	105.9(3)
Co−Se(1)−Mn(1)	80.94(6)	Co−Se(1)−C(21)	112.1(3)
Co−Se(2)−Mn(1)	82.41(6)	Co−Se(2)−C(27)	116.6(3)
Co−Se(3)−Mn(1)	81.69(6)	Co−Se(3)−C(33)	107.1(3)
Te(1)−Co−Te(2)	85.17(5)	Te(1)−Co−Se((1)	96.55(6)
Te(1)−Co−Se(2)	88.77(6)	Te(1)−Co−Se(3)	173.18(6)
Te(1)−Co−C(1)	95.0(3)	Te(2)−Co−Se(1)	174.80(6)
Te(2)−Co−Se(2)	91.59(6)	Te(2)−Co−Se(3)	96.12(6)
Te(2)−Co−C(1)	90.9(3)	Se(1)−Co−Se(2)	83.56(6)
Se(1)−Co−Se(3)	81.61(6)	Se(1)−Co−C(1)	93.8(3)
Se(2)−Co−Se(3)	84.51(6)	Se(2)−Co−C(1)	175.6(3)
Se(3)−Co−C(1)	91.7(3)	Se(1)−Mn(1)−Se(2)	80.99(6)
Se(1)−Mn(1)−Se(3)	79.00(6)	Se(2)−Mn(1)−Se(3)	81.35(6)
Te(1)−Mn(2)−Te(2)	82.09(6)		

(b) $(CO)_3Mn(\mu\text{-}SePh)_3Fe(CO)_3$

Fe−Se(1)	2.449(1)	Fe−Se(2)	2.461(1)
Fe−Se(3)	2.444(1)	Mn−Se(1)	2.477(1)
Mn−Se(2)	2.502(1)	Mn−Se(3)	2.492(1)
Se(1)−C(7)	1.953(7)	Se(2)−C(13)	1.917(8)
Se(3)−C(19)	1.937(7)		

Se(1)−Fe−Se(2)	80.59(4)	Se(1)−Fe−Se(3)	83.48(4)
Se(2)−Fe−Se(3)	82.27(4)	Se(1)−Mn−Se(2)	79.24(4)
Se(1)−Mn−Se(3)	81.92(4)	Se(2)−Mn−Se(3)	80.51(4)
Fe−Se(1)−Mn	82.68(4)	Fe−Se(2)−Mn	81.92(4)
Fe−Se(3)−Mn	82.48(5)	C(1)−Fe−C(2)	96.4(4)
C(1)−Fe−C(3)	93.6(4)	C(2)−Fe−C(3)	94.5(3)
C(4)−Mn−C(5)	90.9(4)	C(4)−Mn−C(6)	91.7(4)
C(5)−Mn−C(6)	87.3(4)		

Table 5. Fractional Atomic Coordinates and B_{eq} Values (Å^2) for *cis*-[PPN][$Mn(CO)_4(SePh)_2$][a]

	x	*y*	*z*	B_{eq}[b]
Mn	0.7914(3)	0.4549(3)	0.24437(12)	4.75(19)
Se(1)	0.7945(3)	0.6571(3)	0.31015(9)	5.92(15)
Se(2)	0.6776(3)	0.5362(3)	0.18655(10)	7.10(18)
C(1)	0.6247(24)	0.355(3)	0.2587(9)	7.6(17)
C(2)	0.8777(25)	0.4148(23)	0.2893(8)	6.2(16)
C(3)	0.784(3)	0.3113(23)	0.1958(8)	6.7(17)
C(4)	0.9490(24)	0.582(3)	0.2264(9)	6.9(16)
C(5)	0.8217(22)	0.6159(20)	0.3756(6)	4.6(13)
C(6)	0.9497(21)	0.7038(24)	0.4062(8)	6.6(15)
C(7)	0.960(3)	0.674(3)	0.4544(8)	9.1(21)
C(8)	0.854(3)	0.562(3)	0.4699(8)	7.8(20)
C(9)	0.7403(23)	0.4839(23)	0.4368(8)	6.1(15)
C(10)	0.7176(22)	0.5083(23)	0.3922(7)	5.8(15)
C(11)	0.7346(22)	0.4937(24)	0.1193(7)	5.7(15)
C(12)	0.819(3)	0.596(3)	0.0967(8)	7.3(17)
C(13)	0.849(3)	0.561(3)	0.0506(8)	8.4(21)
C(14)	0.802(3)	0.430(3)	0.0234(8)	8.2(19)
C(15)	0.718(3)	0.322(3)	0.0439(9)	9.7(19)
C(16)	0.6775(24)	0.355(3)	0.0922(8)	7.3(15)
O(1)	0.5069(19)	0.2936(20)	0.2707(7)	10.5(14)
O(2)	0.9306(16)	0.3856(16)	0.3171(5)	7.1(11)
O(3)	0.7865(22)	0.2195(17)	0.1680(6)	10.0(15)
O(4)	1.0504(18)	0.6673(20)	0.2157(7)	9.9(14)

[a] Esd's refer to the last digit printed. [b] $B_{eq} = {}^8/_3\pi^2\sum_i\sum_j U_{ij}a_i^*a_j^*a_ia_j$.

moderately air-sensitive crystals from THF−hexane under CO atmosphere at −10 °C and could be stored infinitely under CO

Table 6. Fractional Atomic Coordinates and B_{eq} Values (Å^2) for [Na-18-crown-6-ether][$(CO)_3Mn(\mu\text{-}SeMe)_3Mn(CO)_3$][a]

	x	*y*	*z*	B_{eq}[b]
Se	0.07104(7)	0.16049(7)	0.14826(3)	2.96(5)
Mn(1)	0	0	0.09704(6)	2.56(7)
Mn(2)	0	0	0.19882(6)	2.72(7)
C(1)	0.1254(6)	0.0642(7)	0.06596(22)	3.1(5)
C(2)	0.1267(7)	0.0655(7)	0.22908(22)	3.6(5)
C(3)	0.2398(6)	0.2380(7)	0.1492(3)	4.1(5)
O(1)	0.2037(5)	0.1040(5)	0.04419(17)	4.9(4)
O(2)	0.2066(5)	0.1065(6)	0.25063(18)	5.8(4)

[a] Esd's refer to the last digit printed. [b] $B_{eq} = {}^8/_3\pi^2\sum_i\sum_j U_{ij}a_i^*a_j^*a_ia_j$.

Table 7. Fractional Atomic Coordinates and B_{eq} Values (Å^2) for $(CO)_4Mn(\mu\text{-}TePh)_2Co(CO)(\mu\text{-}SePh)_3Mn(CO)_3$[a]

	x	*y*	*z*	B_{eq}[b]
Te(1)	0.67830(7)	0.41032(6)	0.37842(5)	3.75(4)
Te(2)	0.59129(7)	0.41734(7)	0.18078(5)	4.70(4)
Se(1)	0.89220(9)	0.11505(9)	0.32517(7)	3.07(5)
Se(2)	0.59982(10)	0.17203(9)	0.33014(7)	3.60(5)
Se(3)	0.80433(10)	0.12237(9)	0.14578(7)	3.26(5)
Co	0.75082(13)	0.26925(12)	0.25322(9)	3.26(7)
Mn(1)	0.77181(15)	−0.00343(14)	0.28284(10)	3.68(9)
Mn(2)	0.56421(15)	0.58471(14)	0.28205(12)	4.23(10)
C(1)	0.8672(9)	0.3296(9)	0.1942(7)	3.8(6)
C(2)	0.7344(10)	−0.0734(9)	0.3871(8)	4.8(7)
C(3)	0.8987(10)	−0.1233(10)	0.2519(7)	4.8(7)
C(4)	0.6773(10)	−0.0667(9)	0.2416(7)	4.4(6)
C(5)	0.4165(10)	0.5555(11)	0.3378(8)	6.0 (8)
C(6)	0.4918(11)	0.6928(10)	0.2094(9)	5.8(8)
C(7)	0.7159(10)	0.6071(9)	0.2341(8)	5.0(7)
C(8)	0.5435(10)	0.6872(10)	0.3620(8)	5.4(7)
C(9)	0.8311(9)	0.4696(8)	0.3885(7)	3.8(6)
C(10)	0.9495(10)	0.4127(9)	0.3512(7)	4.3(6)
C(11)	1.0420(10)	0.4608(10)	0.3555(8)	5.2(7)
C(12)	1.0161(11)	0.5598(10)	0.3966(9)	6.2(8)
C(13)	0.8975(11)	0.6132(10)	0.4355(9)	6.0(8)
C(14)	0.8040(10)	0.5693(9)	0.4327(8)	4.8(7)
C(15)	0.6839(10)	0.4479(10)	0.0525(7)	4.9(6)
C(16)	0.6780(12)	0.3800(12)	−0.0118(9)	7.2(10)
C(17)	0.7382(16)	0.3888(15)	−0.0953(9)	10.8(14)
C(18)	0.7999(16)	0.4650(16)	−0.1197(10)	11.3(14)
C(19)	0.8042(17)	0.5362(17)	−0.0606(10)	12.9(15)
C(20)	0.7450(14)	0.5269(13)	0.0264(8)	8.6(10)
C(21)	0.8585(9)	0.1315(8)	0.4498(7)	4.1(6)
C(22)	0.7579(10)	0.1129(9)	0.5100(7)	4.7(6)
C(23)	0.7456(10)	0.1165(10)	0.6000(7)	4.9(7)
C(24)	0.8343(11)	0.1382(10)	0.6315(8)	5.6(8)
C(25)	0.9361(12)	0.1572(10)	0.5719(8)	6.0(8)
C(26)	0.9465(10)	0.1532(9)	0.4823(7)	4.6(6)
C(27)	0.4677(9)	0.1789(8)	0.2731(7)	3.9(6)
C(28)	0.3576(11)	0.1851(12)	0.3270(8)	6.5(8)
C(29)	0.2589(11)	0.1845(13)	0.2964(10)	8.3(10)
C(30)	0.2699(11)	0.1776(12)	0.2086(10)	8.1(11)
C(31)	0.3792(12)	0.1704(13)	0.1523(9)	7.7(10)
C(32)	0.4804(10)	0.1706(11)	0.1855(8)	6.2(8)
C(33)	0.9763(10)	0.1015(9)	0.0886(7)	4.0(6)
C(34)	1.0714(11)	0.0218(10)	0.1151(8)	5.4(7)
C(35)	1.1925(11)	0.0127(11)	0.0670(8)	6.6(8)
C(36)	1.2136(11)	0.0819(12)	−0.0031(8)	6.4(8)
C(37)	1.1215(12)	0.1625(11)	−0.0293(8)	6.7(9)
C(38)	0.9991(11)	0.1728(10)	0.0174(7)	5.3(7)
O(1)	0.9420(7)	0.3669(7)	0.1531(5)	6.0(5)
O(2)	0.7109(9)	−0.1219(7)	0.4534(5)	7.5(6)
O(3)	0.9790(7)	−0.2061(7)	0.2337(5)	6.2(5)
O(4)	0.6183(7)	−0.1112(7)	0.2172(6)	6.3(5)
O(5)	0.3279(7)	0.5349(9)	0.3684(7)	9.0(7)
O(6)	0.4477(9)	0.7620(8)	0.1624(7)	9.3(7)
O(7)	0.8074(7)	0.6258(7)	0.2069(5)	6.2(5)
O(8)	0.5300(7)	0.7533(7)	0.4126(6)	7.2(6)

[a] Esd's refer to the last digit printed. [b] $B_{eq} = {}^8/_3\pi^2\sum_i\sum_j U_{ij}a_i^*a_j^*a_ia_j$.

atmosphere in THF, permitting full characterization by IR, ^{1}H NMR, elemental analysis, and X-ray diffraction (Figure 1). The complex *cis*-$[Mn(CO)_4(SePh)_2]^-$ is intensely colored, presum-

Table 8. Fractional Atomic Coordinates and B_{eq} Values (Å^2) for $(CO)_3Mn(\mu\text{-}SePh)_3Fe(CO)_3$[a]

	x	*y*	*z*	B_{eq}[b]
Fe	0.65880(12)	0.53633(6)	0.20995(6)	3.21(5)
Mn	0.93161(12)	0.40769(6)	0.24975(7)	3.28(6)
Se(1)	0.64780(9)	0.40240(4)	0.25121(5)	3.28(4)
Se(2)	0.89089(9)	0.53377(4)	0.31180(5)	3.52(4)
Se(3)	0.84296(9)	0.48597(4)	0.13160(5)	3.48(4)
C(1)	0.5055(10)	0.5257(5)	0.1279(5)	4.6(5)
C(2)	0.7071(9)	0.6341(5)	0.1907(5)	4.2(4)
C(3)	0.5273(9)	0.5619(4)	0.2744(5)	3.7(4)
C(4)	1.1313(10)	0.4240(5)	0.2480(5)	4.9(5)
C(5)	0.9785(9)	0.3509(4)	0.3340(5)	4.3(4)
C(6)	0.9332(9)	0.3209(5)	0.1952(5)	4.0(4)
C(7)	0.5382(8)	0.3378(4)	0.1685(5)	3.6(4)
C(8)	0.4380(10)	0.2858(5)	0.1915(6)	5.7(5)
C(9)	0.3537(12)	0.2376(5)	0.1362(7)	7.3(6)
C(10)	0.3700(13)	0.2439(6)	0.0607(7)	7.2(6)
C(11)	0.4695(12)	0.2957(5)	0.0394(5)	6.4(6)
C(12)	0.5568(10)	0.3419(5)	0.0926(5)	5.0(5)
C(13)	0.8107(8)	0.5308(5)	0.4070(4)	3.7(4)
C(14)	0.7645(12)	0.5990(5)	0.4353(6)	5.7(5)
C(15)	0.7012(12)	0.6010(6)	0.5011(6)	6.7(6)
C(16)	0.6884(13)	0.5355(7)	0.5434(5)	6.9(6)
C(17)	0.7382(12)	0.4689(6)	0.5170(6)	7.0(6)
C(18)	0.7986(11)	0.4655(5)	0.4495(6)	5.9(5)
C(19)	0.9782(9)	0.5694(4)	0.1118(5)	3.7(4)
C(20)	1.0986(10)	0.5982(5)	0.1668(5)	4.8(5)
C(21)	1.1900(11)	0.6582(5)	0.1481(7)	6.7(6)
C(22)	1.1611(14)	0.6869(6)	0.0759(8)	7.4(7)
C(23)	1.0417(14)	0.6597(6)	0.0200(6)	7.7(7)
C(24)	0.9481(11)	0.5996(6)	0.0396(5)	6.4(5)
O(1)	0.4098(7)	0.5206(4)	0.0753(4)	7.0(4)
O(2)	0.7389(7)	0.6959(3)	0.1790(4)	6.7(4)
O(3)	0.4405(7)	0.5789(3)	0.3131(3)	5.5(3)
O(4)	1.2624(7)	0.4332(4)	0.2468(4)	7.3(4)
O(5)	1.0156(7)	0.3104(4)	0.3865(4)	6.6(4)
O(6)	0.9352(7)	0.2631(3)	0.1636(4)	6.6(4)

[a] Esd's refer to the last digit printed. [b] $B_{eq} = {}^8/_3\pi^2\sum_i\sum_j U_{ij}a_i^*a_j^*a_ia_j$.

ably due to the chalcogen to Mn(I) charge transfer excitation. In the UV−visible region *cis*-$[Mn(CO)_4(SePh)_2]^-$ does not exhibit ligand-field transitions. At room temperature, *cis*-$[Mn(CO)_4(SePh)_2]^-$ in THF solution lost CO to form bezeneselenolate-triply-bridged $[(CO)_3Mn(\mu\text{-}SePh)_3Mn(CO)_3]^-$. This transformation occurred slowly in ambient temperature over 48 h, during which period no intermediate was detected spectrally (Scheme 1b).

To evaluate the influence of Se−Se bond strength of diorganyl diselenides on oxidative addition to $[Mn(CO)_5]^-$ [16] and the reactivity of *cis*-$[Mn(CO)_4(SeR)_2]^-$ (R = Ph, Me) which may be tailored by pendant ligand selection, the attempted synthesis of *cis*-$[Mn(CO)_4(SeMe)_2]^-$ in a manner analogous to that for *cis*-$[Mn(CO)_4(SePh)_2]^-$ by reaction of 1 equiv of $[Mn(CO)_5]^-$ and 1 equiv of $(MeSe)_2$ was investigated in THF around −20 °C. The IR spectrum (ν(CO) (THF): 2114 w, 2027 s, 1998 m cm^{-1}, C_{4v} pattern) in the carbonyl stretching region in the course of the reaction between $[Mn(CO)_5]^-$ and $(MeSe)_2$ clearly indicated the presence of an intermediate, presumably **A**.

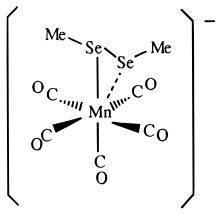

A

When the temperature of the reaction mixture was raised to 25 °C, the carbonyl stretching bands (2114 w, 2027 s, 1998 m cm^{-1} (THF)) almost completely disappeared, followed by formation of a new four-band pattern (2031 w, 1960 s, 1938 m, 1894 m cm^{-1} (THF)) in the IR ν_{CO} region. The single ^{1}H NMR resonance (δ 1.53 (s) ppm (CD_3CN)) observed for $-CH_3$ ligands suggested equivalent methaneselenolate environments, and its upfield chemical shift (vs $(MeSe)_2$) provided the evidence for formation of manganese(I) methaneselenolate. ^{1}H NMR and IR measurements of ν_{CO} showed formation of orange solid *cis*-$[Mn(CO)_4(SeMe)_2]^-$. The general reaction shown in Scheme 1a with diphenyl diselenide appears to be valid for dimethyl diselenide; however, reaction of $[Mn(CO)_5]^-$ and $(MeSe)_2$ is slower. Upon being stirred for extended periods under CO atmosphere in THF at ambient temperature, a solution of *cis*-$[Mn(CO)_4(SeMe)_2]^-$ converted into a red-brown solution. The ^{1}H NMR and IR (ν_{CO}) spectra and X-ray diffraction revealed the complex to be a methaneselenolate-triply-bridged dimer of composition $[(CO)_3Mn(\mu\text{-}SeMe)_3Mn(CO)_3]^-$ (Figure 2). These results show the relative order of thermal stability of anionic manganese(I)−selenolate complexes is *cis*-$[Mn(CO)_4(SePh)_2]^-$ > *cis*-$[Mn(CO)_4(SeMe)_2]^-$, implying that a more electron-donating ligand destabilizes the monomeric manganese(I)−selenolate−carbonyl complexes.

As a part of comprehensive exploration of metal chalcogenolates, we examined the reactivity of manganese−selenolate species *cis*-$[Mn(CO)_4(SeR)_2]^-$ (R = Ph, Me) and attempted to synthesize heterometallic mixed-chalcogenolate complexes by adopting *cis*-$[Mn(CO)_4(SeR)_2]^-$ as a precursor. *cis*-$[Mn(CO)_4(SePh)_2]^-$ and *cis*-$[Mn(CO)_4(TePh)_2]^-$ were reacted in stoichiometric proportions with $Co(ClO_4)_2\cdot 6H_2O$ and $(PhSe)_2$ (1:1:1:0.5 molar ratio) in THF under a nitrogen atmosphere, and the reaction mixture finally led to the isolation of the dark purple heterometallic mixed chalcogenolate $(CO)_4Mn(\mu\text{-}TePh)_2Co(CO)(\mu\text{-}SePh)_3Mn(CO)_3$ (Scheme 1e). Here the *cis*-$[Mn(CO)_4(SePh)_2]^-$ and *cis*-$[Mn(CO)_4(TePh)_2]^-$ are able to act as "chelating metallo ligands" for a Co^{2+} species.[17] The proposed mechanism is shown in Scheme 2; oxidation of Co^{2+} of the coordination compound $(CO)_4Mn(\mu\text{-}TePh)_2Co^{II}(\mu\text{-}SePh)_2Mn(CO)_4$ by diphenyl diselenide led to the presumed intermediate $(CO)_4Mn(\mu\text{-}TePh)_2Co(SePh)(\mu\text{-}SePh)_2Mn(CO)_4$, and subsequent rearrangement of the terminal benzeneselenolate ligand to bridge two metals and shift of a labile carbonyl from Mn(I) to Co(III) yielded neutral $(CO)_4Mn(\mu\text{-}TePh)_2Co(CO)(\mu\text{-}SePh)_3Mn(CO)_3$.[17c] The result clearly indicated that the reaction pathway in Scheme 2a is adopted instead of the pathway in Scheme 2b. The formation of the complex $(CO)_4Mn(\mu\text{-}TePh)_2Co(CO)(\mu\text{-}SePh)_3Mn(CO)_3$ provides insight into the preferred stereochemistry of Co(III)−selenolate−tellurolate complexes, and the mechanism is relevant to the oxidative Bennett approach using $(RS)_2$ and Co^{2+}.[18] The light- and air-sensitive $(CO)_4Mn(\mu\text{-}TePh)_2Co(CO)(\mu\text{-}SePh)_3Mn(CO)_3$, which is stable in nonpolar hexane−ether, was easily crystallized from ether−hexane at −10 °C and partially decomposed into insoluble solid in THF−CH_3CN overnight at room temperature. The ^{1}H and ^{13}C NMR spectra of $(CO)_4Mn(\mu\text{-}TePh)_2Co(CO)(\mu\text{-}SePh)_3Mn(CO)_3$ shows the expected signals (^{1}H NMR (C_4D_8O) δ 6.95−8.24 (m) ppm;

(16) Treichel, P. M.; Nakagaki, P. C. *Organometallics* **1986**, *5*, 711.
(17) (a) White, G. S.; Stephan, D. W. *Inorg. Chem.* **1985**, *24*, 1499. (b) Wark, T. A.; Stephan, D. W. *Inorg. Chem.* **1990**, *29*, 1731. (c) Waldbach, T. A.; van Rooyen, P. H.; Lotz, S. *Angew. Chem., Int. Ed. Engl.* **1993**, *32*, 710.
(18) (a) Lane, R. H.; Bennett, L. E. *J. Am. Chem. Soc.* **1970**, *92*, 1089. (b) Asher, L. E.; Deutsch, E. *Inorg. Chem.* **1975**, *14*, 2799. (c) Weschler, C. J.; Deutsch, E. *Inorg. Chem.* **1973**, *12*, 2682. (d) Lane, R. H.; Sedor, F. A.; Gilroy, M. J.; Eisenhardt, P. F.; Bennett, L. E. *Inorg. Chem.* **1977**, *16*, 93. (e) Dickman, M. H.; Doedens, R. J.; Deutsch, E. *Inorg. Chem.* **1980**, *19*, 945. (f) Koch, S.; Tang, S. C.; Holm, R. H.; Frankel, R. B. *J. Am. Chem. Soc.* **1975**, *97*, 914.

Scheme 1

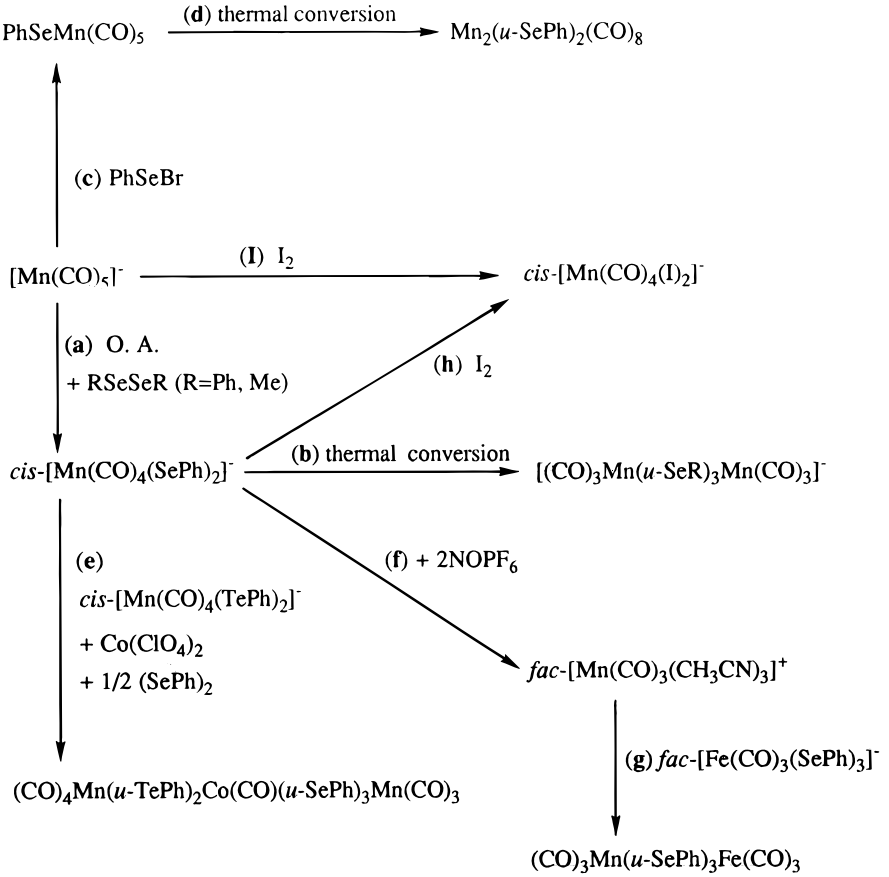

Scheme 2

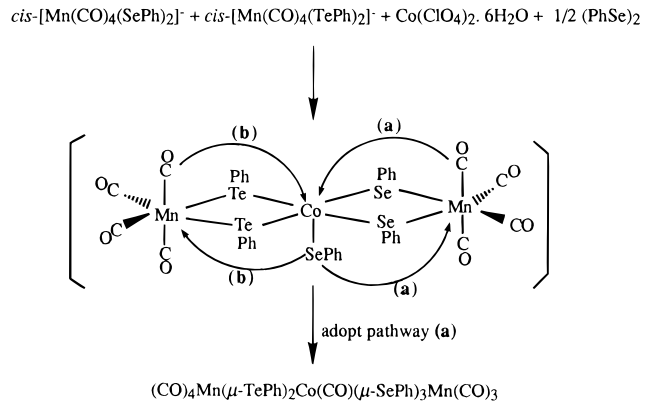

^{13}C NMR (C_4D_8O) δ 129.0−138.4 (m) ppm) for the phenyl ligands involved and display characteristics of diamagnetic d^6 Co(III) and d^6 Mn(I) species.

To evaluate the influence of the more electron-donating groups on the reactivity with Co^{2+}, we surveyed the reactivity of dimethyl diselenide toward $Co(ClO_4)_2 \cdot 6H_2O$ in the presence of *cis*-$[Mn(CO)_4(SeMe)_2]^-$ (eq 1). An immediate reaction

$$2cis\text{-}[Mn(CO)_4(SeMe)_2]^- + Co(ClO_4)_2 \cdot 6H_2O + {}^1/_2(MeSe)_2 \rightarrow (CO)_4Mn(\mu\text{-}SeMe)_2Co(CO)(\mu\text{-}SeMe)_3Mn(CO)_3 \quad (1)$$

ensued under the same reaction conditions. The IR carbonyl stretching (2068 w, 2027 sh, 1998 vs, 1981 sh, 1961 w, 1917 m cm^{-1} (THF)) and ^{1}H NMR (C_4D_8O) (δ 2.20 (s), 2.00 (s), 1.93 (s), 1.86 (s), 1.57 (s) ppm) and ^{13}C NMR (C_4D_8O) (δ 5.88 (s), 4.99 (s), 3.41 (s), 3.36 (s), 2.20 (s) ppm) spectra confirm the formation of the neutral $(CO)_4Mn(\mu\text{-}SeMe)_2Co(CO)(\mu\text{-}SeMe)_3Mn(CO)_3$. No decomposition was observed in THF at room temperature for 3 days. However, when attempting to isolate the analogue $(CO)_4Mn(\mu\text{-}SePh)_2Co(CO)(\mu\text{-}SePh)_3Mn(CO)_3$ by drying under vacuum and extracting with diethyl ether, we isolated only an insoluble dark solid. It seems that the strongly basic chelating metallo ligand *cis*-$[Mn(CO)_4(SeMe)_2]^-$ can better stabilize the trinuclear Mn(I)−Co(III)−Mn(I)−chalcogenolate complex than the weakly basic chelating metallo ligand *cis*-$[Mn(CO)_4(SePh)_2]^-$. In brief, the electronic and solvent effects play important roles in stabilizing the Mn(I)−Co(III)−Mn(I)−chalcogenolate complexes.

The chemical oxidation of *cis*-$[Mn(CO)_4(SePh)_2]^-$ with oxidants was investigated. It was hoped that one-electron oxidation would lead to formation of an Se−Se bond that would likely undergo an aggregation process resulting in higher nuclearity species. Unfortunately, with the addition of 2 equiv of $NOPF_6$ to 1 equiv of *cis*-$[Mn(CO)_4(SePh)_2]^-$ in CH_3CN at room temperature, the identifiable products are the well-known *fac*-$[Mn(CO)_3(CH_3CN)_3]^+$ along with $(PhSe)_2$, identified by ^{1}H NMR and gas chromatography (Scheme 1f).[11] The oxidation process was also investigated using I_2 as the oxidant. Dropwise addition of I_2 solution to a solution of *cis*-$[Mn(CO)_4(SePh)_2]^-$ in THF at room temperature produced the isostructural product *cis*-$[Mn(CO)_4(I)_2]^-$, on the basis of the infrared carbonyl stretching spectra, and $(PhSe)_2$, characterized by ^{1}H NMR and GC.[12] Presumably, the reaction undergoes reductive elimination followed by oxidative addition (Scheme 1h).

The anionic $[(CO)_3Mn(\mu\text{-}SeR)_3Mn(CO)_3]^-$ (R = Ph, Me) feature octahedral coordination about each of the two Mn(I) ions with three terminal carbonyls in the facial positions and bear a closer structural resemblance to the recently reported $[Fe(CO)_3(SePh)_3Na \cdot 3THF]$ in which the d^6 Fe(II) $[Fe(CO)_3]^+$ fragment is isolobal with the d^6 Mn(I) $[Mn(CO)_3]^+$ fragment

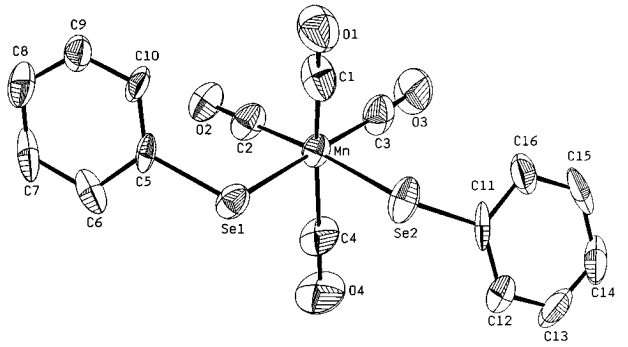

Figure 1. ORTEP drawing and labeling scheme of the *cis*-$[Mn(CO)_4(SePh)_2]^-$ anion with thermal ellipsoids drawn at the 50% probability level.

of $[(CO)_3Mn(\mu\text{-}SeR)_3Mn(CO)_3]^-$.[1b] Attempts to prepare a heterometallic manganese−iron−selenolate complex in a straightforward manner by the simple salt elimination reaction between *fac*-[PPN][$Fe(CO)_3(SePh)_3$] and *fac*-$[Mn(CO)_3(CH_3CN)_3][PF_6]$ led to the neutral $(CO)_3Mn(\mu\text{-}SePh)_3Fe(CO)_3$ in THF (Scheme 1g). The IR carbonyl stretching (ν(CO) (THF): 2081 m, 2031 sh, 2017 s, 1931 s cm^{-1}) and ^1H NMR spectra (δ (CD_3CN) 7.27−8.02 (m) ppm) are consistent with the presence of the low-spin octahedrally coordinated d^6 Fe(II) and d^6 Mn(I) ions with facial carbonyls. The light-sensitive, thermally unstable $(CO)_3Mn(\mu\text{-}SePh)_3Fe(CO)_3$ was formed as dark brown-red crystals in good yield after recrystallization from diethyl ether. X-ray diffraction confirmed the formation of $(CO)_3Mn(\mu\text{-}SePh)_3Fe(CO)_3$, which is isostructural with $[(CO)_3Mn(\mu\text{-}SeMe)_3Mn(CO)_3]^-$ (Figure 4). In light of these results, this synthetic procedure proved useful in the preparation of heterometallic chalcogenolates.

Structure. Due to the facile CO lability of *cis*-$[Mn(CO)_4(SePh)_2]^-$, an atmosphere of CO was present to force the formation of *cis*-[PPN][$Mn(CO)_4(SePh)_2$] crystals over that of the CO loss product $[(CO)_3Mn(\mu\text{-}SePh)_3Mn(CO)_3]^-$ at −10 °C. The crystal structure of *cis*-[PPN][$Mn(CO)_4(SePh)_2$]·2THF consists of well-separated cations and anions and two THF solvent molecules; there are no exceptional cation−anion interactions. The PPN^+ cations show the expected geometry. The manganese ion in complex **1** is surrounded in a distorted octahedral fashion by two terminal benzeneselenolate groups and four carbonyls with a bond angle of 82.97(13)° for Se(1)−Mn−Se(2) (Figure 1). Inspection of the angle between *cis*-benzeneselenolate-coordination sites highlights the extent to which the molecule is distorted. This acute angle appears to result from intramolecular interaction of the two selenium sp^3 lone pairs. Surprisingly, two carbonyl ligands (C(4)−O(4) and C(1)−O(1)) tilt toward the benzeneselenolates (Se(2)−Mn−C(4) 83.6(8)°, Se(2)−Mn−C(1) 85.1(9)°). These Mn−Se distances (2.529(4) and 2.524(4) Å) in **1** are much shorter than the terminal Mn−Se bonds in the anion $[Mn(SePh)_4]^{2-}$ (average 2.567 Å)[19] but longer than the terminal Mn−Se bonds in Mn-$(SeC_6H_3\text{-}2,6\text{-}Mes_2)_2\cdot 2CH_2Cl_2$ (2.498(1) Å).[3c] The Se(1)···Se(2) contact distance (3.347(4) Å) in **1** shows no formal Se−Se bond; however, this contact distance is inside of the sum of the van der Waals radii (4.0 Å).[20] A comparison of the structure of complex **1** with its previously published Te analogue *cis*-[Mn-$(CO)_4(TePh)_2]^-$ reveals a very close correspondence of structural details.[2] The Mn−Te bond lengths in *cis*-$[Mn(CO)_4(TePh)_2]^-$ are 0.146 Å longer than those of Mn−Se in **1**, and the bond angle 82.97(13)° for Se−Mn−Se in **1** is slightly larger than the 82.79(4)° Te−Mn−Te bond angle in *cis*-$[Mn(CO)_4(TePh)_2]^-$, which might be accredited to the longer Mn−Te bonds. The presumed delocalized pairs of electrons along Se−Mn−Se in **1** reflects the tetrahedral array around the selenium atoms with Mn−Se(1)−C(5) 104.1(5)° and Mn−Se(2)−C(11) 105.6(6)°.

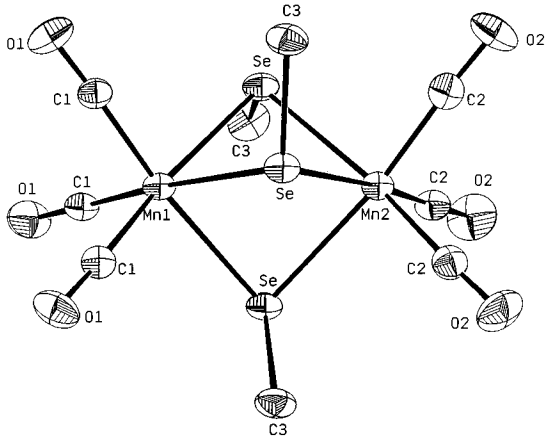

Figure 2. ORTEP drawing and labeling scheme of the $[(CO)_3Mn(\mu\text{-}SeMe)_3Mn(CO)_3]^-$ anion with thermal ellipsoids drawn at the 50% probability level.

The structure of $[(CO)_3Mn(\mu\text{-}SeMe)_3Mn(CO)_3]^-$ is shown in Figure 2. Table 3 gives a listing of significant bond lengths and angles for complex **2**. The anion **2** contains two Mn atoms, and each is coordinated by three terminal CO ligands and three bridging MeSe ligands. To a first approximation, the $MnSe_3(CO)_3$ framework may be described as face-sharing octahedra. The methyl groups of three bridging μ_2-methaneselenolates in **2** form a regular propeller-like arrangement around the Se_3 plane defined by the three seleniums. $[(CO)_3Mn(\mu\text{-}SeMe)_3Mn(CO)_3]^-$ contains dinuclear units in which Mn(I) centers are unsymmetrically bridged by three μ_2-methaneselenolates. The Mn(1)−Se bonds of average length 2.508(3) Å are 0.012 Å longer than Mn(2)−Se bonds (average distance 2.496(3) Å). The μ_2-bridging Mn−Se bonds of average length 2.502(3) Å in **2** are 0.112 Å shorter than bridging Mn−Se bonds (average distance 2.614(2) Å) in $[Mn\{N(SiMe_3)_2\}(\mu\text{-}SeC_6H_2\text{-}i\text{-}Pr_3\text{-}2,4,6)\cdot THF]_2$.[21]

An ORTEP projection of the neutral trinuclear $(CO)_4Mn(\mu\text{-}TePh)_2Co(CO)(\mu\text{-}SePh)_3Mn(CO)_3$ is shown in Figure 3. The selected bond distances and angles are listed in Table 4. Complex **3** has a linear chain of two Mn atoms and one Co atom; the central cobalt ion is bridged by two benzenetellurolates, three benzeneselenolates, and a terminal CO, thus completing the octahedral coordination sphere of the Co(III) ion. While one of the two outer Mn ions is coordinated by three terminal carbonyls and three bridging PhSe ligands, another Mn atom is coordinated by two bridging PhTe ligands and four terminal carbonyls. Overall, the geometry around each of three metals may be described as a distorted octahedron. The Co(III)−Se distances observed in **3** (average 2.450(2) Å) are much longer than that observed in $[(en)_2Co(SeCH_2CH_2NH_2)][(NO_3)_2]$ (2.378(1) Å).[22] The Co(III)−Te bond distances of 2.576(2) Å (average) are slightly shorter than those in the recently reported $(CO)_4Mn(\mu\text{-}TePh)_2Co(CO)(\mu\text{-}TePh)_3Mn(CO)_3$ (average distance 2.589(5) Å);[2] however, they are comparable with the Co(I)−Te bond distance of 2.543(1) Å in $Co(TeSi(SiMe_3)_3)(PMe_3)_3$.[23] The longer Co(III)−CO bond distance

(19) Tremel, W.; Krebs, B.; Greiwe, K.; Simon, W.; Stephan, H. O.; Henkel, G. *Z. Naturforsch., B* **1992**, *47B*, 1580.
(20) (a) Pauling, L. *The Nature of the Chemical Bond*, 2nd ed.; Cornell University Press: Ithaca, NY, 1960; p 260. (b) Wolmershäuser, G.; Heckmann, G. *Angew. Chem., Int. Ed. Engl.* **1992**, *31*, 779.
(21) Bochmann, M.; Powell, A. K.; Song, X. *Inorg. Chem.* **1994**, *33*, 400.
(22) Stein, C. A.; Ellis, P. E.; Elder, R. C., Jr.; Deutsch, E. *Inorg. Chem.* **1976**, *15*, 1618.

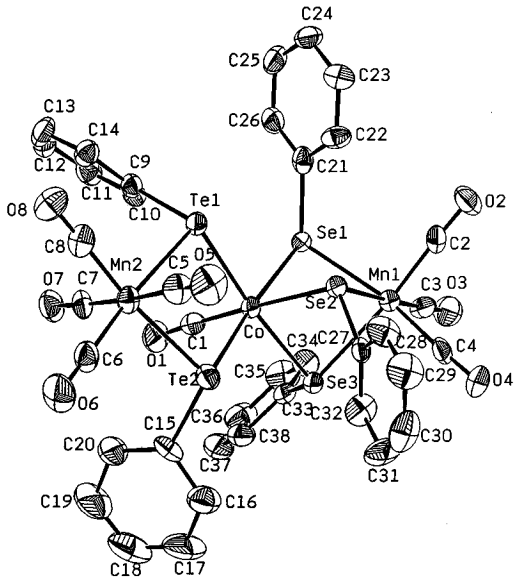

Figure 3. ORTEP drawing and labeling scheme of neutral $(CO)_4Mn(\mu\text{-}TePh)_2Co(CO)(\mu\text{-}SePh)_3Mn(CO)_3$ with thermal ellipsoids drawn at the 50% probability level.

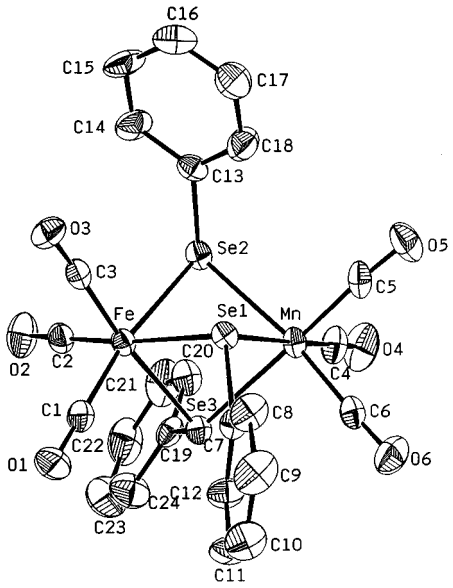

Figure 4. ORTEP drawing and labeling scheme of neutral $(CO)_3Mn(\mu\text{-}SePh)_3Fe(CO)_3$ with thermal ellipsoids drawn at the 50% probability level.

(1.761(10) Å) observed in **3** compared with the Co(III)−CO bond distance 1.75(3) Å in $(CO)_4Mn(\mu\text{-}TePh)_2Co(CO)(\mu\text{-}TePh)_3Mn(CO)_3$ is, presumably, ascribed to the weaker σ-donating ability of benzeneselenolate *trans* to the Co−CO bond (bond angle Se(2)−Co−C(1) 175.6(3)°). It is not surprising that the bite angle Te(1)−Co−Te(2) of the "chelate $(CO)_4Mn(\mu\text{-}TePh)_2$" is 85.17(5)° in **3**, which is slightly larger than the Se−Co−Se average angle of 83.23(6)°. The Te(1)−Mn(2)−Te(2) bond angle (82.09(6)°) in **3** is comparable with the Te−Mn−Te bond angle, 82.79(4)°, in starting material *cis*-$[Mn(CO)_4(TePh)_2]^-$. The selenium atoms of the triply-bridging benzeneselenolates adopt a severely distorted tetrahedral arrangement of three bonding pairs and one lone pair of electrons because of the sharp Co−Se−Mn bridge angles (average Mn−Se−Co bond angle 81.68(6)°).

The molecular structure of the neutral $(CO)_3Mn(\mu\text{-}SePh)_3Fe(CO)_3$ with the atomic numbering scheme is shown in Figure 4, with selected bond lengths and angles given in Table 4. In a sense, neutral complex **4** is isostructural with the anion $[(CO)_3Mn(\mu\text{-}SeMe)_3Mn(CO)_3]^-$. Compound **4** contains discrete dinuclear units in which the d^6 Fe(II) and d^6 Mn(I) ions are unsymmetrically bridged by three benzeneselenolates. The average Fe−SePh bond length of 2.451(1) Å in **4** is comparable with the reported terminal Fe−SePh bond length of 2.459(2) Å in *fac*-$[Fe(CO)_3(SePh)_3]^-$,[1b] 2.460(12) Å in tetrahedral $[Fe(SePh)_4]^{2-}$,[24] and 2.421(1) Å in $Fe(Se\text{-}2,6\text{-}i\text{-}Pr_2C_6H_3)_2(PMe_2Ph)_2$.[25] Oddly, the bridging Mn−Se distances (average 2.490(1) Å) are marginally (ca. 0.037 Å) shorter than the terminal Mn−Se bond distances in **1**. The Se−Fe(II)−Se angles average 82.11(4)°, which is significantly larger than the Se−Mn(1)−Se angles (average 80.56(4)°). It is possible that the larger Se−Fe(II)−Se angle is due to the proximity of the bridging-benzeneselenolate groups to the Fe(II) center. The C−Fe(II)−C bond angles (average 94.8(4)°) are also larger than the C−Mn(I)−C bond angles (average 90.0(4)°) observed in **4**.

Conclusion. The syntheses of new Mn(I)−selenolate complexes, *cis*-$[Mn(CO)_4(SeR)_2]^-$ (R = Ph, Me) and $[(CO)_3Mn(\mu\text{-}SeR)_3Mn(CO)_3]^-$, have been achieved by oxidative addition of $(RSe)_2$ to *cis*-$[Mn(CO)_5]^-$ and thermal transformation of *cis*-$[Mn(CO)_4(SeR)_2]^-$, respectively. Our efforts also have been directed to clarify the course of reactions (oxidative addition vs nucleophilic displacement) in reactions of *cis*-$[Mn(CO)_5]^-$ with $(RSe)_2$ and PhSeBr individually. Concerning reactivities of *cis*-$[Mn(CO)_4(SeR)_2]^-$ and *fac*-$[Fe(CO)_3(SePh)_3]^-$, we showed that *cis*-$[Mn(CO)_4(SeR)_2]^-$ and *fac*-$[Fe(CO)_3(SePh)_3]^-$ act as "chelating metallo ligands" in the syntheses of the heterometallic chalcogenolate compounds $(CO)_4Mn(\mu\text{-}TePh)_2Co(CO)(\mu\text{-}SePh)_3Mn(CO)_3$ and $(CO)_3Mn(\mu\text{-}SePh)_3Fe(CO)_3$. We also made a comparison between "chelating metallo ligands" *cis*-$[Mn(CO)_4(SeMe)_2]^-$ and *cis*-$[Mn(CO)_4(SePh)_2]^-$ in light of chelating ability; the electronic and solvent effects play crucial roles in stabilizing the mixed-metal Mn(I)−Co(III)−Mn(I)−chalcogenolate complexes.

Acknowledgment. We thank the National Science Council of the Republic of China (Taiwan) for support of this work.

Supporting Information Available: Tables of crystal data and experimental conditions for the X-ray studies, atomic coordinates and B_{eq} values, bond lengths and angles, and anisotropic temperature factors for *cis*-$[Mn(CO)_4(SePh)_2]^-$, $[(CO)_3Mn(\mu\text{-}SeMe)_3Mn(CO)_3]^-$, $(CO)_4Mn(\mu\text{-}TePh)_2Co(CO)(\mu\text{-}SePh)_3Mn(CO)_3$, and $(CO)_3Mn(\mu\text{-}SePh)_3Fe(CO)_3$ (25 pages). Ordering information is given on any current masthead page.

IC951487T

(23) Gindelberger, D. E.; Arnold, J. *Inorg. Chem.* **1993**, *32*, 5813.
(24) McConnachie, J. M.; Ibers, J. A. *Inorg. Chem.* **1991**, *30*, 1770.
(25) Forde, C. E.; Morris, R. H.; Ramachandran, R. *Inorg. Chem.* **1994**, *33*, 5647.